Water Practice & Technology

IWA PUBLISHING

Water Practice & Technology Vol 18 No 5, 1172 doi: 10.2166/wpt.2023.065

An improved technique for reducing water wastage from micro-RO-membrane-based water purification systems: An experimental study

Ravi Kiran Varma and Jaideep Chatterjee*

Department of Chemical Engineering, BITS-Pilani, Hyderabad Campus, Medchal, Telangana 500078, India
*Corresponding author. E-mail: jaideepc@hyderabad.bits-pilani.ac.in

RKV, 0000-0003-1527-6627; JC, 0000-0003-1034-5961

ABSTRACT

While reverse osmosis (RO) has emerged as the leading technology for home-use and point-of-use (POU) water purification, this technology leads to water wastage as the reject. This wastage needs to be reduced, especially in water-stressed regions of the world. In this paper, we report an experimental study, which demonstrates that it is possible to operate a home-use RO-based water purification system, at ~75% recovery, without significantly compromising the life of the membrane. The membrane element is 'cleaned' using a hydrostatic and osmotically driven backwash using the permeate produced in the system. This study examines the effect of the permeate volume used for the backwash, on the extent of salt removal from the membrane module. During this study, which involved the measurement of the total dissolved solids (TDS) of the backwash-effluent, it was observed that the backwash-effluent showed dual-minima in the effluent TDS. This paper further examines this dual-minima observed under different experimental conditions. Data generated suggest the causes for the dual-minima.

Key words: high-recovery RO, home-use water purifier, osmotic backwash, POU water purification

HIGHLIGHTS

- Water savings from reverse osmosis systems.
- Scale prevention in RO membranes.
- Dual-minima in backwash TDS.
- Backwash optimization.

GRAPHICAL ABSTRACT

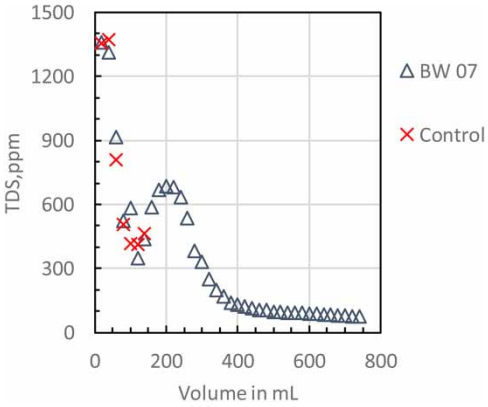

INTRODUCTION

Point-of-use (POU) water purification for home-use drinking water purification has grown significantly in parts of the world including India, in the past two decades. Several technologies, including ultra-violet (UV) radiation, chlorine-based disinfection, filtration using activated carbon, and media made of polymeric fibers, have been

used in these home-use water purification systems. However, small reverse osmosis (RO)-based water purification systems (micro-scale RO purifiers) have emerged as the most-favored technology, with or without some of the other technologies mentioned. One of the major advantages of RO-based systems is the discernable 'improvement' in the taste of water due to the reduction of dissolved ions in water. This taste change assures the user that the water is purified or 'improved' compared to other technologies, such as UV-based disinfection, which do not produce a discernable taste improvement in the product water. It is also known that RO removes pathogenic bacteria, viruses, other micro-organisms, dissolved organics, pesticides, and dissolved ions from drinking water. Some of the ions removed such as arsenic, lead, mercury, nitrates, and fluorides are known to be detrimental to human health and are occasionally present at dangerous levels in groundwater sources. Other ions removed, such as iron and aluminum, are not desirable in drinking water due to health-related or esthetic reasons. Some ions removed such as sodium, potassium, calcium, magnesium, and chlorides may be required by the human body, but these are also available from other inexpensive food sources. In addition, the amount of these ions, available from drinking water, may not be sufficient to meet our nutritional needs, hence their removal is often tolerable, given the huge benefits arising from the removal of the toxic ions and pathogenic micro-organisms. Finally, drinking water is consumed to meet our need for hydration and not for nutrition. The above benefits have made RO technology the clear front-runner for home-use and POU water purification systems.

However, the home-use RO technology has a clear negative, which is the considerable volume of water wasted as the 'reject'. This problem is enhanced by consumers and manufacturers choosing to operate the water purifiers at a recovery of 10–40%. This is done to prevent scale formation and hence irreversible membrane fouling. Membrane damage due to scaling requires the replacement of the most expensive component of the water purification system, which is the RO membrane element. Hence, a technology for automated membrane cleaning that allows the water purifier to be operated at ~75% pure water recovery, without significantly compromising the membrane life, could lead to significant water saving at the national and international levels. This study results from an ongoing program, which is developing technologies that will enable the operation of home-use RO purification systems at near ~75% recovery of product water.

The following aspects of home-use RO-based water purifiers which make them distinct from other continuously operated, larger RO-based water purification systems, must be kept in mind, to appreciate this work. First, home-use RO-based water purification systems are not continuously operated, since the typical requirement of a family, for drinking water, is met within an hour of operation of the purification system. Hence, a typical purification system is on stand-by mode for ~23 h/day. Some larger systems could be on stand-by mode for ~8 h between cycles of operation. Second, the power consumption of a typical RO-based home-use water purification system is quite low (~30 W), in comparison to other home appliances, such as modern TVs (40–65 W), ceiling fans (75 W), and room lights (60–10 W). Hence, a small increase in the same, while it is in use, would not impact the users of the technology.

Osmotic backwash in continuous RO membrane filtration processes has been proposed and applied previously (Sagiv & Semiat 2005; Avraham *et al.* 2006; Qin *et al.* 2010). Various studies of the osmotic backwash of RO membranes and UF membranes in large-scale desalination systems have been reported (Nam *et al.* 2012; Ramon *et al.* 2013; Gilabert-Oriol *et al.* 2014; Kim 2014; Park *et al.* 2014; Jiang *et al.* 2015; Gao *et al.* 2016). Several studies have reported the use of osmotic backwash for maintaining flux in forward osmosis (FO) systems (Blandin *et al.* 2016; Gwak & Hong 2017; Motsa *et al.* 2017), which are typically used for energy recovery from wastewater. Even in these systems with high organic fouling potential, osmotic backwashing showed positive results. Warsinger *et al.* (2018) reported a study of osmotic backwash on a batch RO system, wherein they found that, if the residence time of the high-concentration feed, is kept below the 'induction time' for crystallization, scale formation can be effectively prevented. Dana *et al.* (2019) reported a study of osmotic backwashing of RO and NF membranes used for brackish and wastewater treatment and found that sulphate-based solutions have a better ability to maintain the permeate flux by cleaning the $CaPO_4$ scale. Yaranal *et al.* (2020) studied pressure-assisted osmotic (PAO) backwash for RO membrane modules, in which backwashing was achieved by pressurizing the permeate, in addition to permeate flow, due to the osmotic potential. Lee *et al.* (2021) compared 'salt' cleaning and osmotic backwash in lab-scale nano-filtration membranes and found that due to the ion exchange of the Ca ions with Na ions, the integrity of the fouling layer is weakened. Simple physical cleaning using feed water and/or permeate has been reported in several studies. Oh *et al.* (2009) studied scale formation on RO membranes due to the precipitation of calcium salts. The study found that while surface nucleation dominates, bulk crystallisation is also responsible for scale formation. Ma *et al.* (2013) reported a study of backwashing of fouled

UF membranes, using both UF permeate and RO permeate, and found that better results were achieved when backwash was performed with RO permeate. Zhang *et al.* (2015) reported a study of cleaning membranes used for membrane distillation. Chemical-based cleaning has been reported in several studies (Ferrer *et al.* 2015; Lee *et al.* 2017a, 2017b), in which sodium hypochlorite has been used, occasionally in combination with HCl. Some papers (Al-Ghamdi *et al.* 2019; Alpatova *et al.* 2020) have investigated a unique backwashing approach using an aqueous solution of CO_2, wherein the gas nucleates as the pressure drops, forming bubbles, which dislodge the foulants on the membrane surface. More recent studies have explored the use of ultra-sonication (Hube *et al.* 2023), 'water-hammer' type effects induced by pressure variations (Aslam *et al.* 2022), and other novel chemical means for the prevention of membrane fouling (Khan *et al.* 2023; Qiao *et al.* 2023).

During the study, reported in this paper, which involved the measurement of the total dissolved solids (TDS) of the backwash-effluent, it was observed that the gravity and osmotically driven backwash-effluent showed a dual-minima in the effluent TDS (Figures 6(a) and (b) and 7(a) and (b)). Such an observation has not been reported earlier, to the best of our knowledge. These observations were studied under multiple operating conditions, to understand the causes for the dual-minima. The above observations can be used to optimize the gravity and osmotically driven backwash system. The membrane element is 'cleaned' using a gravity and osmotically driven backwash using the permeate produced by the system. This study examines the effect of the permeate volume used for the backwash, on the extent of residual salt removal from the membrane module.

MATERIALS AND METHODS

A schematic of the apparatus used as the experimental 'control' in this study, is shown in Figure 1. The input water used in this study is the tap water supplied at the University (BITS-Pilani, Hyderabad Campus) which is a mixture of the water supplied by the Hyderabad Metropolitan Water Supply and Sewerage Board (HMWSSB) and local groundwater supplied by bore-wells in the campus. A complete analysis of the local groundwater is shown in Supplementary material, Appendix 1. An analysis of the tap water used is shown in Supplementary material, Appendix 2. It may be noted that while there is some seasonal variation in the water quality, we do not expect its quality to change significantly over the course of this study. The HMWSSB obtains fresh water from water reservoirs located near the city of Hyderabad, which are naturally filled by rainwater from their catchment areas during the monsoon months (June–September). The water from these freshwater reservoirs have lower TDS and hardness as compared to the groundwater sources mentioned above. The use of 'tap water' is preferred over synthetic water, since in the experience of the authors, fouling of water purifier components may be better simulated with the natural water supply. Another advantage of using tap water is that the disposal of the concentrate from the experiment does not pose any risk to the environment, since no synthetic salts are added to the water.

The experiments were performed in the following manner, using the parts described in the following paragraphs. Tap water discussed above is allowed into the experimental control apparatus, shown in Figure 1, at the point labeled 1. This water is routed through a manual valve (2) and a pre-filter casing (4), which holds a pre-filter (3) made of polymeric fibers. This pre-filter was replaced at regular intervals due to fouling by colloids

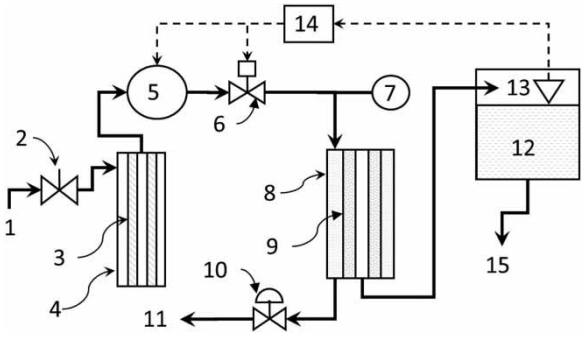

Figure 1 | Schematic of the experimental system used as the experimental 'control'. (1) Water supply; (2) manual shut-off valve; (3) filter; (4) filter casing; (5) pump; (6) shut-off valve; (7) pressure gauge; (8) RO membrane casing; (9) RO membrane; (10) throttle valve; (11) discharge to sink; (12) storage tank; (13) level controller; (14) switch; and (15) discharge port.

and bio-fouling. The output from the pre-filter was connected to a positive displacement pump (5). The pump (BNQS DP-125-100-1) 125 psi, manufactured by Ningbo Qiansheng Electric Motor Company Limited, China, was procured locally in Hyderabad, India. Downstream of the pump is a solenoid valve (6), which is connected to the RO membrane casing (8). The pump (5) and the solenoid valve (6) are powered by the same power supply (2-A, 24-Volt DC) (14). The RO membrane elements (9) were DOW FILMTEC (BW6-1812-75), RO membrane modules, manufactured by The DOW Chemical Company, USA, and procured locally in Hyderabad, India. These spiral wound membranes were fitted in the membrane casing (8). The reject/concentrate outlet port of the membrane casing is connected to a throttle value (10), which is used to control the operating pressure on the feed side of the membrane casing. The pressure is measured using the pressure gage (7), fitted at the feed end of the membrane casing. The discharge (11) of the reject downstream of the throttle value is available for measurements and is disposed of to the sink. The permeate from the membrane casing is discharged into the permeate collection tank (12). During the regular batch mode operation of the above RO system, the volumetric flow rate of the permeate (Q_P) and the volumetric flow rate of the reject (Q_R) were measured. The recovery (Y) was estimated from the above values, using the following equation.

$$Y = \frac{Q_P}{Q_T} \tag{1}$$

where Q_P refers to the permeate flow rate and Q_T refers to total flow rate.

The throttle valve (10) ensured that the recovery was maintained as ~75% during the experiment. The TDS of the input tap water, the permeate TDS, and the reject-TDS, were also measured, which were used to estimate recovery, using the following equation, obtained from the steady-state material balance.

$$Y = \frac{C_R - C_F}{C_R - C_P} \tag{2}$$

where C_R refers to the reject-TDS (mg/L); C_F refers to the feed TDS (mg/L); C_P refers to the permeate TDS.

The estimate of recovery from the above validated the recovery estimate from the flow rates. A level control element (13) in the permeate collection tank is used to cut-off power to the power supply (14), which shuts off the pump and the solenoid valve, when the permeate tank is filled to capacity (~25 L), thereby mimicking the batch-operating mode of most POU and home-use drinking water purification systems. The closure of the solenoid valve (6) prevents water from draining out of the membrane cartridge (8). At this point in time, the small volume of water, entrained in the RO casing, is discharged through the reject line (11). This discharge-water from the reject line after shut-down was collected at regular time intervals, and its volume and TDS were measured. These values are reported and discussed in the subsequent sections. All material parts used above were procured individually, which are available as spare parts in the Indian market.

A schematic of the experimental system, which was tested for its ability to enhance life of the RO membrane, when the system is operated for ~75% recovery, is shown in Figure 2. All parts were identical to the experimental control, shown in Figure 1, expect for a small vertical cartridge (16), which was placed in the permeate line

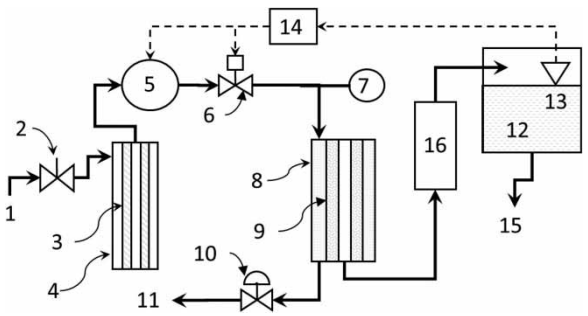

Figure 2 | Schematic of the experimental system tested in this study to enhance the 'life' of the RO membrane element. (1) Water supply; (2) manual shut-off valve; (3) filter; (4) filter casing; (5) pump; (6) shut-off valve; (7) pressure gauge; (8) RO membrane casing; (9) RO membrane; (10) throttle valve; (11) discharge to sink; (12) storage tank; (13) level controller; (14) switch; (15) discharge port; and (16) backwash permeate holding chamber.

downstream of the RO membrane casing, but upstream of the permeate collection tank (12). The internal capacity of this 'intermediate' permeate holding tank (16) can vary between 100 mL and 1 L, the optimization of which, was one of the objectives of this study. The permeate entered the small reservoir cartridge (16) from the bottom and exited the same from its top, during normal operation of the RO system. With this arrangement of the parts, the permeate from the RO element, first filled-up this small 'intermediate' permeate reservoir, before reaching the main permeate reservoir (12) and filling the same. During the experiment, the system was powered on, with the permeate storage tank empty. While the system was in operation, the permeate volumetric flow rate (Q_P) and the reject volumetric flow rate, Q_R, were measured, and the recovery was estimated, based on these values. The recovery was maintained ~75% during the experiment, using the throttle valve (10). The TDS of the permeate, the TDS of the reject, and the TDS of the input tap water were measured, and these values are reported in the subsequent sections. The system was allowed to run, till the permeate storage tank was filled to capacity, which caused the system to shut-off. In this system also, the closure of the solenoid valve (6) prevented the drainage of water from the RO casing. The post-shut-down water collected from the reject discharge port (11), in this system, is called the 'backwash' water, whose TDS and volume were carefully measured over time and are reported in the subsequent sections.

DATA AND OBSERVATIONS

The experimental control apparatus, shown in Figure 1, was operated to fill the storage tank (12), which had a capacity of ~25 L. This is termed as one operating cycle. One operating cycle lasted for ~1 h at the beginning and increased to 4 h after ~30 cycles. The post-shut-down discharge-water was collected from the reject port (11), for measurements. The system was allowed to be on stand-by for at least 1 h, during which the permeate storage tank was drained. Typically, the operating cycles of the 'control' experiment (Figure 1) and the experimental system (Figure 2) were performed alternately. The operating cycle for the experimental system was followed by the 'backwash', which lasted longer. The typical 'cycle time' for the experimental system was shorter than the above and increased from ~1 h, at the start to ~2 h after ~30 cycles. A life-time experiment lasted for ~40 cycles.

Figure 3(a) shows a comparison of the permeate flow rate of the 'control' and the experimental systems, with the total volume of input water through these systems. Figure 3(b) shows a comparison of the above data, with the number of operating cycles. It can be observed that the permeate flow rate decline of the experimental system was significantly lower than the permeate flow rate decline in the 'control'. Figure 3(c) shows a comparison of the cycle time of the 'control' and the experimental systems, with the number of cycles. It can be observed that the time required to produce 25 L of the permeate increased from 1 to 4 h, for the control and to 2 h in the experimental system. The recovery of permeate, maintained during the above experiments, over the total volume of water purified, is shown in Figure 3(d). It can be seen that the recovery in the experimental system was held at ~80% over the experiment, while the recovery in the control system could not be maintained due to excessive scaling in the same.

Figure 4(a) shows the variation in the TDS of the feed water, the reject water, and the permeate, for the 'control'. Figure 4(b) shows the variation of TDS values measured, for the 'experimental' system. It may be noted that the TDS of the input water remained between 200 and 300 ppm, while the TDS of the reject exceeded 1,000 ppm, due to the high recovery maintained during these experiments. It can also be observed that the permeate TDS in both systems, remained well below 100 ppm, indicating that the RO membrane elements were performing as designed. In order to better understand the causes for the enhanced life of the RO membrane in the experimental system, compared to the control, a detailed study of the membrane module backwash was conducted and is described in the following paragraphs.

It was observed that when an operating cycle for the 'control' got over, a small volume of water is discharged from the RO membrane casing, through the reject line. A fixed volume (20 mL) of this discharge-water was collected, and its TDS was measured. The total volume of the discharge-water was ~140 mL. The TDS of the discharge-water declined with time and with discharge volume. While the flow rate of the discharge declined with time, it continued to 'drip-out' for ~2 h after shut-off. Figure 5(a) shows the measured variation of the TDS of this discharge with the volume of the discharge, while Figure 5(b) shows the variation in the discharge-water TDS with time, from the instant of shut-off (zero-time). The data are shown for three experimental runs, where the maximum reject-TDS measured were similar (discharge run 1; discharge run 5; discharge run 10). Figure 5(c) shows the estimated mass of salts removed from the RO membrane casing, by the

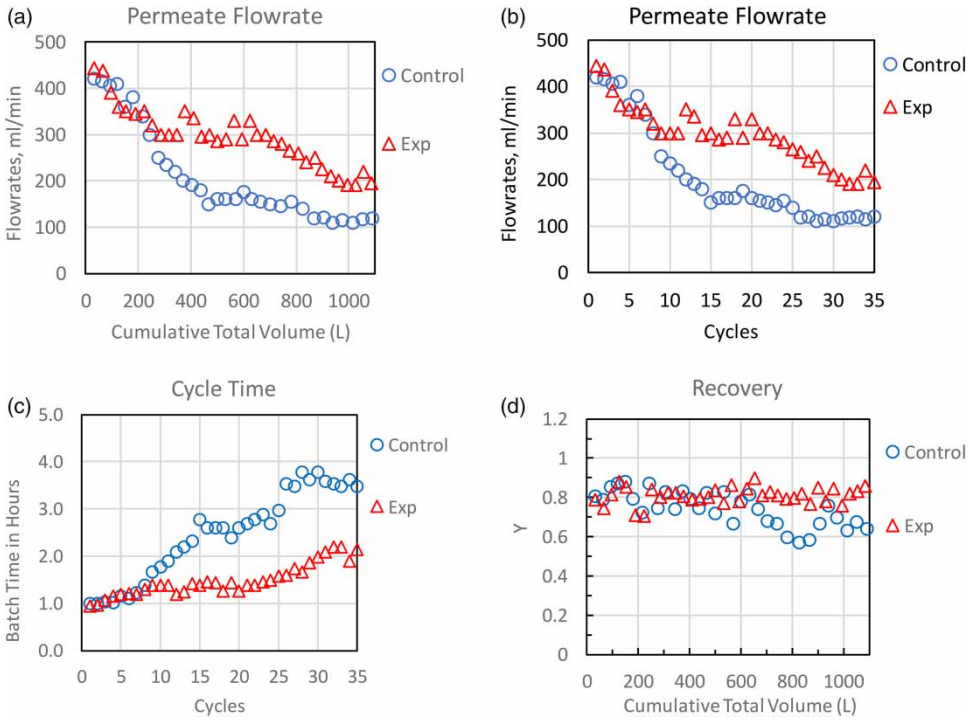

Figure 3 | (a) Measured variation in the permeate flow rate with total volume of water purified, for the experimental (Δ) and the control (*O*) configurations. (b) Measured variation in the permeate flow rate with the number of cycles, for the experimental (Δ) and the control (*O*) configurations. (c) Measured variation in the operating 'cycle time' with the number of cycles, for the experimental (Δ) and the control(*O*) configurations. (d) Measured variation in the recovery with total volume of water purified, for the experimental (Δ) and the control(*O*) configurations.

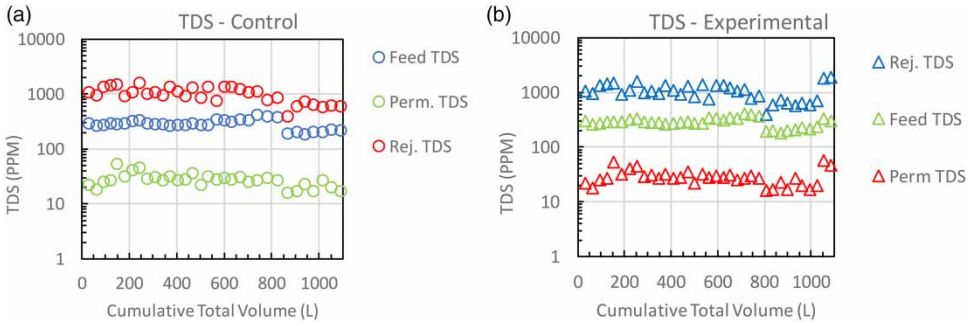

Figure 4 | (a) Measured variation in the TDS of the input water, the permeate, and the reject, for the 'control' configuration. (b) Measured variation in the TDS of the input water, the permeate and the reject, for the 'experimental' configuration.

discharge-water. This mass of salt was estimated by integrating the TDS value over the discharge volume, as shown in the following equation.

$$m_S = \int_0^V c(v)\, dv \tag{3}$$

where m_S refers to the mass of salt removed (mg); c refers to the measured TDS (mg/L); dv refers to the incremental volume collected (mL). Similar observations were made for all 'control' experiments, irrespective of the maximum reject-TDS values encountered.

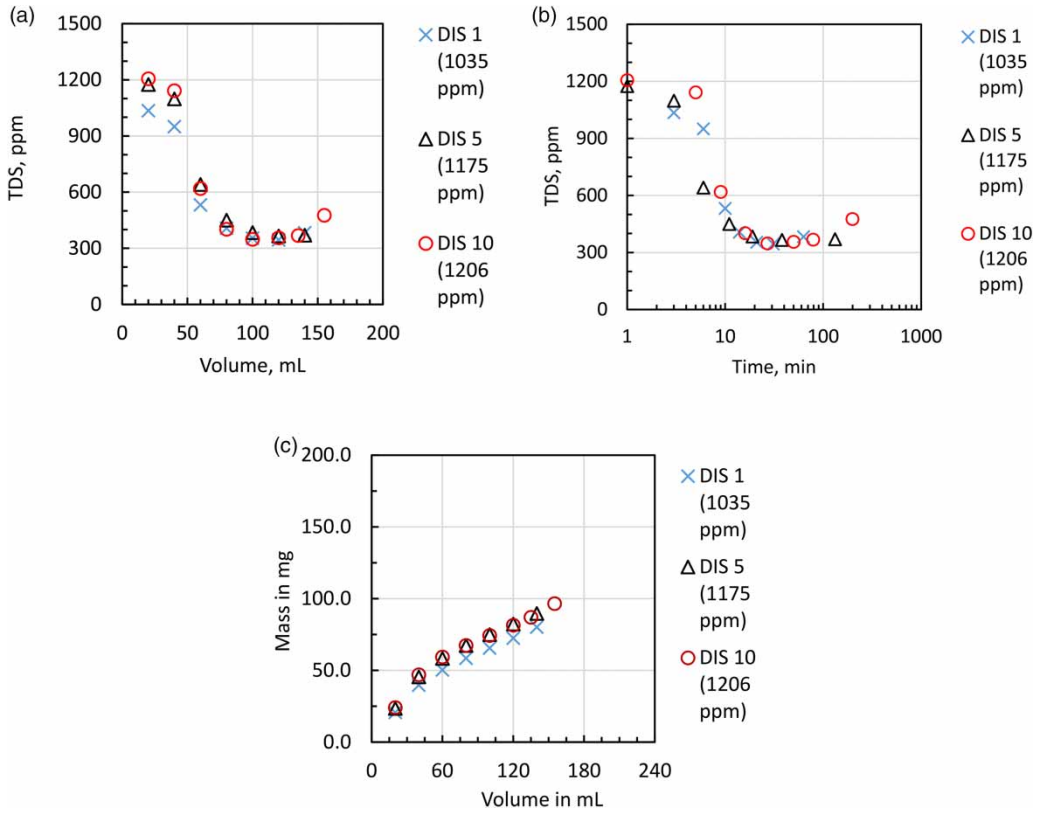

Figure 5 | (a) Measured variation of the discharge-water TDS with the discharge-water volume from the 'control' experiments. These experiments had similar maximum reject-TDS. (b) Measured variation of the discharge-water TDS over the time from shut-off, from the 'control' experiments. These experiments had similar maximum reject-TDS. (c) Estimated variation of the mass of dissolved salts removed with discharge-water volume with the time from shut-off, from the 'control' experiments. These experiments had similar maximum reject-TDS.

Backwash-discharge data, similar to the data shown in Figure 5, was collected from the 'experimental' system. The backwash-discharge data consisted of the time required to collect incremental volume samples of 20 mL, and the TDS in the same. Figure 6(a) shows the measured TDS variation of the backwash-discharge with the volume of this discharge, from the reject line (point 11 in Figure 2). The maximum reject-TDS for these experimental runs were similar. Figure 6(b) shows the measured TDS variation of the 'backwash-discharge' with time, from the point of shut-off, for the same systems. From Figure 6(a), it can be observed that the backwash-discharge TDS variation showed a primary minimum, which occurs after ~100 mL of 'discharge'. From Figure 6(b), it can be observed, that the primary minimum in backwash-discharge TDS occurs after ~10 min of shut-off. This dual-minima in the backwash-discharge-water TDS is of interest and has not been reported earlier, to the best of our knowledge.

The possible causes for the above observations will be discussed in following sections. Figure 6(c) shows the estimated mass of dissolved salts removed from the RO membrane casing, based on Equation (3), during the backwash experiment. Also shown in Figure 6(c) is the mass of dissolved salts removed from the RO membrane casing, which was estimated based on data from a 'control' experiment having similar maximum reject-TDS value. It can be observed that while the 'control' experiment removes about 68 mg of dissolved TDS from the casing, the 'experimental' backwash system is able to remove around 160 mg of dissolved salts.

The backwash-discharge experiments were repeated after multiple operating cycles, where the maximum reject-TDS varied, which occurred due to small changes in input water TDS and adjustments in the recovery, at which the filling cycle was operated. Figure 7(a) shows the measured TDS variation of the backwash-discharge with the volume of this discharge, for the experimental system. The maximum reject-TDS for these experimental runs were ~1,350 ppm. Figure 7(b) shows the measured TDS variation of the backwash-discharge with time, from the point of shut-off, for the same systems. It can be observed, from Figure 7(a), that the backwash-discharge TDS variation showed a primary minimum, which occurs after ~100 mL of 'discharge'. From Figure 7(b), it can be observed that the time at which the primary minimum in the backwash-discharge TDS occurs was ~10 min

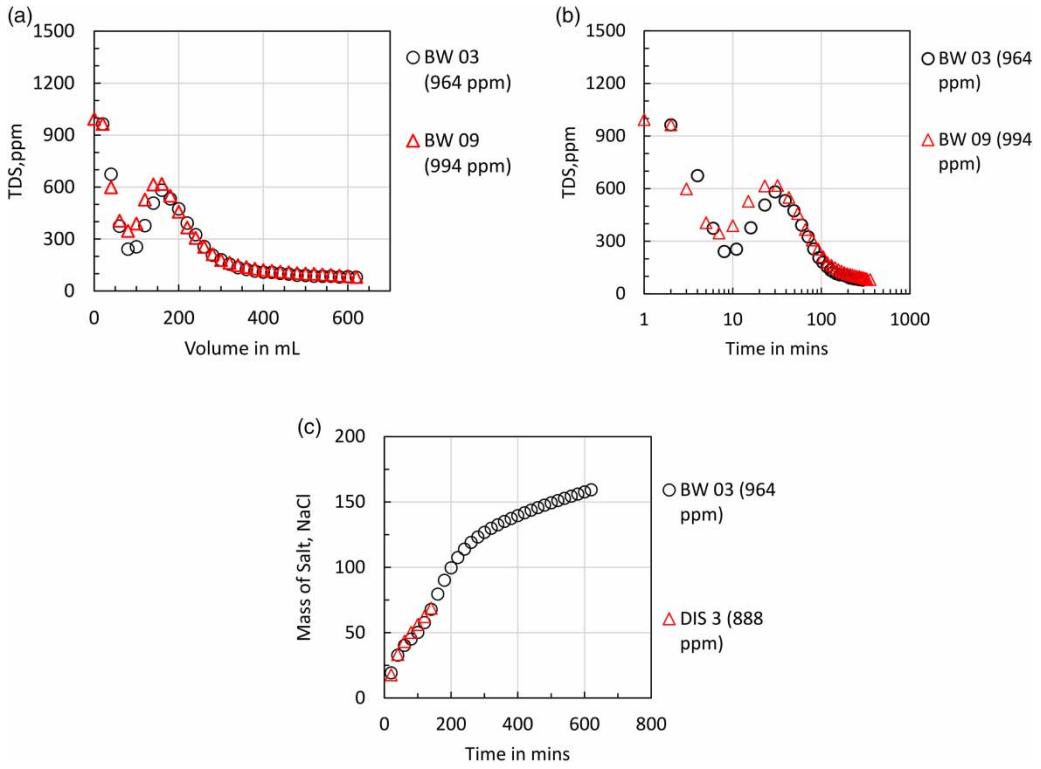

Figure 6 | (a) Measured variation of the backwash-discharge-water TDS over the backwash-discharge-water volume from backwash experiments. These experiments had similar maximum reject-TDS values. (b) Measured variation of the backwash-discharge-water TDS over time, starting from the time of shut-off, from backwash experiments. These experiments had similar maximum reject-TDS values. (c) Estimated variation in the mass of dissolved salts removed from the RO system over the volume of backwash-discharge, from a backwash experiment (O) and a control (Δ) experiment, performed with similar maximum reject-TDS.

from shut-off. Figure 7(c) shows the mass of dissolved salts removed, from the RO membrane casing, which was estimated based on Equation (3), during the backwash experiments. Also shown in Figure 7(d) is the mass of dissolved salts removed from the RO membrane casing, which was estimated from a 'control' experiment having a similar maximum reject-TDS value. It can be observed that while the 'control' experiment removes about 107 mg of dissolved TDS from the RO membrane casing, the 'experimental' backwash system is able to remove around 250 mg of dissolved salts.

RESULTS AND DISCUSSION

The data shown in the previous section suggest the following. First, the experimental system for backwashing, shown in Figure 2, is able to enhance the life of the RO membrane system, when it is operated at a high recovery of ~75%. The TDS data from these 'life-time' experiments demonstrate that the membrane integrity and ability to perform are not compromised by the proposed process of backwash. The above enhancement in life is achieved while using less than 2.5% of the product water for membrane cleaning. The proposed backwashing system is capable of removing 2.5 times higher mass of dissolved salts from the RO membrane element, compared to the 'control' experiment. This mass of salts would have remained within the RO membrane element in the absence of the proposed backwash. The relatively longer time required for the backwash is not an issue with the home-use RO-based water purification systems, as these systems are typically operated for ~1 h/day, spending the remaining 23 h in 'stand-by'.

In the 'control' experiments, the discharge volume of ~150 mL was observed, post-shut-off, which occurs due to the following. The high TDS of water on the feed-reject side of the membrane drains out under the pressure which the membrane was under, at the point of shut-off. This pressure dissipates very quickly post-shut-off, which causes the rapid decline in the discharge flow rate. Since the throttle valve position under the high-recovery operating condition, is almost closed, the discharge occurs slowly, over a period of minutes. The reject water

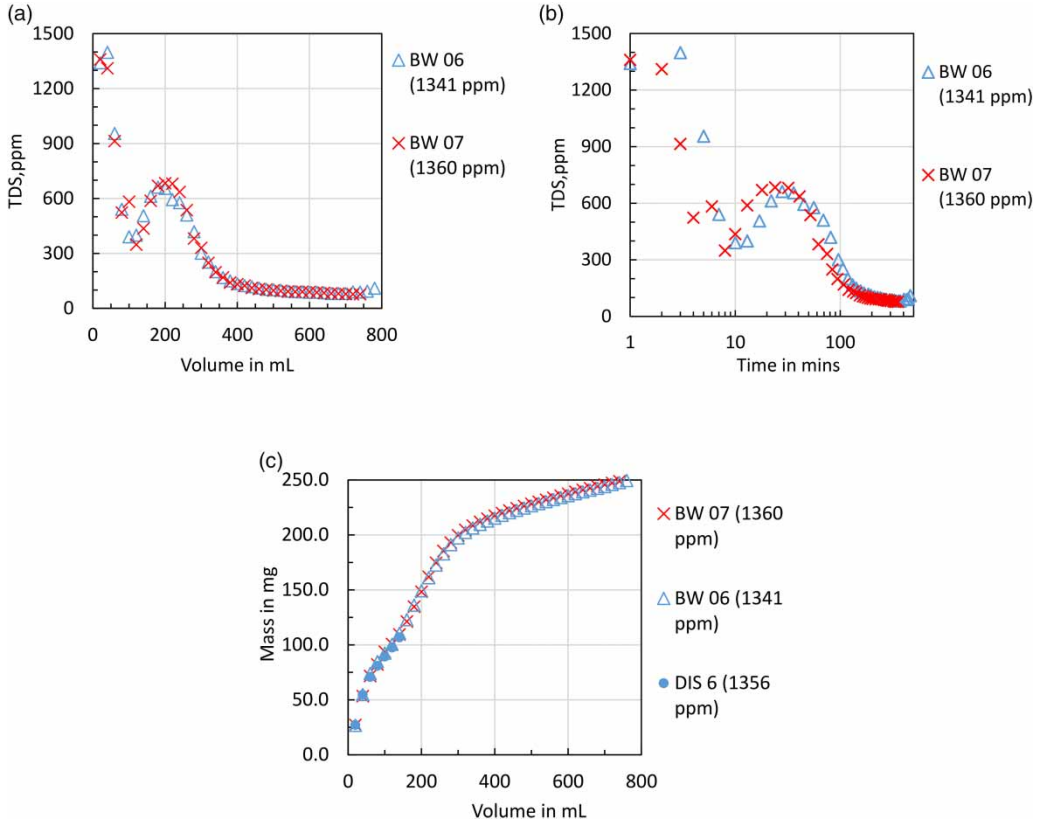

Figure 7 | (a) Measured variation of the backwash-discharge-water TDS over the backwash-discharge-water volume from backwash experiments. These experiments had similar maximum reject-TDS values. (b) Measured variation of the backwash-discharge-water TDS over time, starting from the time of shut-off, from backwash experiments. These experiments had similar maximum reject-TDS values. (c) Estimated variation in mass of dissolved salts removed from the RO module over the volume of backwash-discharge, from Backwash experiments (X, Δ) and a 'control' (*O*) experiment performed with similar maximum reject-TDS.

at the discharge end of the casing is at the highest reject-TDS, while the water at the feed end of the feed-reject side of the membrane is at the feed TDS. Hence, in the control experiments, the TDS of discharge-water can be expected to vary from the maximum reject-TDS to the feed TDS. This is what is experimentally observed and is shown in Figure 5(a) and (b).

The cause of the observed 'dual-minima' in the TDS of the discharge-water, from the experimental system, can be understood, by examining the data shown in Figure 8. Figure 8(a) shows the measured discharge TDS variation from a backwash experiment and from a 'control' experiment conducted under similar conditions (of maximum reject-TDS). It can be observed that the two experimental datasets are almost identical, for up to ~100 mL of discharge volume. In fact, the first minima in TDS can also be observed for the control experiment as well. The control experiment does not have enough permeate, to allow for the 'backwash', which is available in the experimental system. In the experimental system, the permeate collected in the intermediate permeate holding chamber is initially not available for backwash. As the pressure in the membrane casing dissipates post-shut-off, the pressure in the inner core of the membrane element also drops. This drop in pressure in the inner core of the membrane element allows the permeate to flow into the core of the membrane element from the intermediate permeate storage chamber, under gravity. This is the cause for the delay of the backflush which can be observed in the data, shown in the Figures 6–8. FO then draws out the permeate from inside the membrane core to the external part of the membrane casing, from where it flows out through the reject line. The high concentration of the salt present on the membrane surface is the cause of the secondary increase in the backwash-effluent TDS. Eventually, the low TDS permeate is able to displace all high TDS water present on the membrane surface (also called the concentration polarization layer). It can be clearly observed, from Figures 6–8, that at the primary TDS minima, the TDS of the backwash-effluent is the same as the feed water TDS. From the above figures, we observe that the values of the backwash-effluent TDS at the secondary TDS minima are the permeate

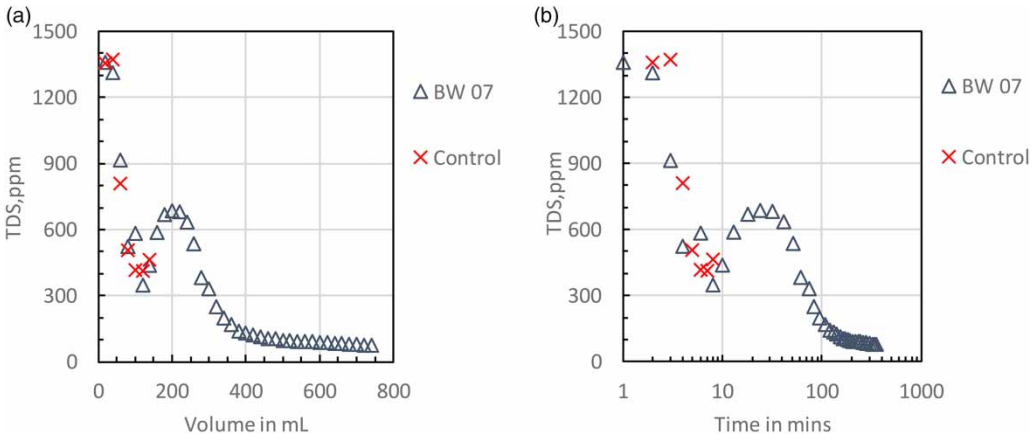

Figure 8 | (a) Comparison of the measured variation of discharge TDS values with volume of discharge, from the experimental (Δ) system and the 'control' (X) system. These experiments had similar maximum reject-TDS (~1,360 ppm). (b) Comparison of the measured variation of discharge TDS values with time from shut-off, from the experimental system (Δ) and the 'control' (X) system. These experiments had similar maximum reject-TDS (~1,360 ppm).

TDS. Without the detailed experimental study reported above, one may be tempted to conclude that the backwash process is only causing the TDS of the water held in the membrane casing, to drop from the feed water TDS to the permeate TDS. However, the secondary peak in the TDS values, observed in Figures 6–8 clearly shows that the above would be erroneous. A much higher mass of salts is washed out of the membrane element due to the backwash process. The above phenomena can be observed in the data presented in Figure 8(b) as well. This figure shows the measured TDS variation with time from the point of 'shut-off', for an experimental backwash system and from an equivalent 'control' experiment (with a similar maximum reject-TDS of ~1,360 ppm). It can be observed that a 'minima' in TDS is observed for both systems, at ~7–8 min. It can be hypothesized, that up to this time, the reject and feed water held in the feed-reject side of the membrane casing is available as discharge. After this point in time, the larger reservoir of permeate becomes available to washout the higher TDS water trapped in the RO membrane element in the casing. The results of this study also point toward the optimal volume of permeate as well as the optimal time for the backwash, by this method. Figures 6(a) and 8(a) suggest that around 400–500 mL of permeate, which is 1.6–2% of the product volume, may be sufficient to backwash the RO membrane element, by the self-cleaning method. Figures 6(b) and 8(b) suggest that a duration of ~2.5 h post-shut-off is required for the backwash-effluent TDS to drop below 100 ppm, which may be the optimal duration between two operating cycles for such systems.

In summary, this experimental study demonstrates a technology which can be used to cause a significant reduction in water wastage from home-use water purification systems, with minimal added parts and cost. It further shows how the volume and time requirements for a complete washout of the RO membrane system can be estimated. It also demonstrates how a significantly higher mass of dissolved salts can be removed from the RO membrane casing by a complete hydrostatic plus osmotic (HPO) backwash. Most importantly, this work demonstrates the risk of retaining a high TDS zone on the membrane surface, when the system goes into stand-by, in the absence of a complete backwash. The observed dual-minima in the backwash-effluent TDS is due to the delay in the reverse flow of the permeate into the membrane core, which is required to trigger forward-osmotically driven backwash. In future research, a mathematical model based on the above will be studied in detail.

ACKNOWLEDGEMENTS

The authors wish to thank BITS-Pilani, Hyderabad Campus, for supporting this study.

DATA AVAILABILITY STATEMENT

All relevant data are included in the paper or its Supplementary Information.

CONFLICT OF INTEREST

J.C., the corresponding author is a 'Technical Expert' for the Water Quality India Association, which represents a group of companies that sell water purification products in South Asia.

REFERENCES

Al-Ghamdi, M. A., Alhadidi, A. & Ghaffour, N. 2019 Membrane backwash cleaning using CO2 nucleation. *Water Res.* **165**, 114985. https://doi.org/10.1016/J.WATRES.2019.114985.

Alpatova, A., Qamar, A., Al-Ghamdi, M., Lee, J. G. & Ghaffour, N. 2020 Effective membrane backwash with carbon dioxide under severe fouling and operation conditions. *J. Membr. Sci.* **611**, 118290. https://doi.org/10.1016/J.MEMSCI.2020.118290.

Aslam, M., Wicaksana, F., Farid, M., Wong, A. & Krantz, W. B. 2022 Mitigation of membrane fouling by whey protein via water hammer. *J. Membr. Sci.* **642**, 119967. https://doi.org/10.1016/J.MEMSCI.2021.119967.

Avraham, N., Dosoretz, C. & Semiat, R. 2006 Osmotic backwash process in RO membranes. *Desalination* **199**, 387–389. https://doi.org/10.1016/J.DESAL.2006.03.088.

Blandin, G., Vervoort, H., Le-Clech, P. & Verliefde, A. R. D. 2016 Fouling and cleaning of high permeability forward osmosis membranes. *J. Water Process Eng.* **9**, 161–169. https://doi.org/10.1016/J.JWPE.2015.12.007.

Dana, A., Hadas, S. & Ramon, G. Z. 2019 Potential application of osmotic backwashing to brackish water desalination membranes. *Desalination* **468**, 114029. https://doi.org/10.1016/J.DESAL.2019.05.012.

Ferrer, O., Lefèvre, B., Prats, G., Bernat, X., Gibert, O. & Paraira, M. 2015 Reversibility of fouling on ultrafiltration membrane by backwashing and chemical cleaning: differences in organic fractions behaviour. *New Pub: Balaban.* **57**, 8593–8607. https://doi.org/10.1080/19443994.2015.1022807.

Gao, L. X., Rahardianto, A., Gu, H., Christofides, P. D. & Cohen, Y. 2016 Novel design and operational control of integrated ultrafiltration – reverse osmosis system with RO concentrate backwash. *Desalination* **382**, 43–52. https://doi.org/10.1016/J.DESAL.2015.12.022.

Gilabert-Oriol, G., Hassan, M., Dewisme, J., Garcia-Molina, V. & Busch, M. 2014 Backwashing pressurized ultrafiltration using reverse osmosis brine in seawater desalination and its potential costs savings. *New Pub: Balaban.* **55**, 2800–2812. https://doi.org/10.1080/19443994.2014.939491.

Gwak, G. & Hong, S. 2017 New approach for scaling control in forward osmosis (FO) by using an antiscalant-blended draw solution. *J. Membr. Sci.* **530**, 95–103. https://doi.org/10.1016/J.MEMSCI.2017.02.024.

Hube, S., Hauser, F., Burkhardt, M., Brynjólfsson, S. & Wu, B. 2023 Ultrasonication-assisted fouling control during ceramic membrane filtration of primary wastewater under gravity-driven and constant flux conditions. *Sep. Purif. Technol.* **310**, 123083. https://doi.org/10.1016/J.SEPPUR.2022.123083.

Jiang, W., Wei, Y., Gao, X., Gao, C. & Wang, Y. 2015 An innovative backwash cleaning technique for NF membrane in groundwater desalination: fouling reversibility and cleaning without chemical detergent. *Desalination* **359**, 26–36. https://doi.org/10.1016/J.DESAL.2014.12.025.

Khan, I. A., Lee, Y. S. & Kim, J. O. 2023 Chemically enhanced pretreatment (CEPT) to reduce irreversible fouling during the clean-in-place process for membranes operating under constant flux and constant pressure filtration. *Desalination* **549**, 116313. https://doi.org/10.1016/J.DESAL.2022.116313.

Kim, S. 2014 Osmotic pressure-driven backwash in a pilot-scale reverse osmosis plant. *New Pub: Balaban.* **52**, 580–588. https://doi.org/10.1080/19443994.2013.826771.

Lee, C. K., Park, C., Choi, J. S. & Kim, J. O. 2017a Effects of various chemical cleaning conditions for pressured MF process. *Water Sci. Technol.* **75**, 1063–1070. https://doi.org/10.2166/WST.2016.573.

Lee, E. S. H., Xiong, J. Y., Han, G., Wan, C. F., Chong, Q. Y. & Chung, T. S. 2017b A pilot study on pressure retarded osmosis operation and effective cleaning strategies. *Desalination* **420**, 273–282. https://doi.org/10.1016/J.DESAL.2017.08.004.

Lee, H., Im, S. J., Lee, H., Kim, C. M. & Jang, A. 2021 Comparative analysis of salt cleaning and osmotic backwash on calcium-bridged organic fouling in nanofiltration process. *Desalination* **507**, 115022. https://doi.org/10.1016/J.DESAL.2021.115022.

Ma, C., Wang, L., Li, S., Heijman, S. G. J., Rietveld, L. C. & Su, X. B. 2013 Practical experience of backwashing with RO permeate for UF fouling control treating surface water at low temperatures. *Sep. Purif. Technol.* **119**, 136–142. https://doi.org/10.1016/J.SEPPUR.2013.08.017.

Motsa, M. M., Mamba, B. B., Thwala, J. M. & Verliefde, A. R. D. 2017 Osmotic backwash of fouled FO membranes: cleaning mechanisms and membrane surface properties after cleaning. *Desalination* **402**, 62–71. https://doi.org/10.1016/J.DESAL.2016.09.018.

Nam, J. W., Park, J. Y., Kim, J. H., Lee, Y. S., Lee, E. J., Jeon, M. J., Kim, H. S. & Jang, A. 2012 Effect on backwash cleaning efficiency with TDS concentrations of circulated water and backwashing water in SWRO membrane. *New Pub: Balaban.* **43**, 124–130. https://doi.org/10.1080/19443994.2012.672162.

Oh, H. J., Choung, Y. K., Lee, S., Choi, J. S., Hwang, T. M. & Kim, J. H. 2009 Scale formation in reverse osmosis desalination: model development. *Desalination* **238**, 333–346. https://doi.org/10.1016/J.DESAL.2008.10.005.

Park, J., Jeong, W., Nam, J., Kim, J., Kim, J., Chon, K., Lee, E., Kim, H. & Jang, A. 2014 An analysis of the effects of osmotic backwashing on the seawater reverse osmosis process. **35**, 1455–1461. https://doi.org/10.1080/09593330.2013.870587.

Qiao, Z., Guo, Y., Wang, Z. & Hu, G. 2023 A chemically enhanced backwash model for predicting the instantaneous transmembrane pressure of flat sheet membranes in constant flow rate mode. *J. Membr. Sci.* **666**, 121137. https://doi.org/10.1016/J.MEMSCI.2022.121137.

Qin, J. J., Oo, M. H., Kekre, K. A. & Liberman, B. 2010 Development of novel backwash cleaning technique for reverse osmosis in reclamation of secondary effluent. *J. Membr. Sci.* **346**, 8–14. https://doi.org/10.1016/J.MEMSCI.2009.08.011.

Ramon, G. Z., Nguyen, T. V. & Hoek, E. M. V. 2013 Osmosis-assisted cleaning of organic-fouled seawater RO membranes. *Chem. Eng. J.* **218**, 173–182. https://doi.org/10.1016/J.CEJ.2012.12.006.

Sagiv, A. & Semiat, R. 2005 Backwash of RO spiral wound membranes. *Desalination* **179**, 1–9. https://doi.org/10.1016/J.DESAL.2004.11.050.

Warsinger, D. M., Tow, E. W., Maswadeh, L. A., Connors, G. B., Swaminathan, J. & Lienhard V, J. H. 2018 Inorganic fouling mitigation by salinity cycling in batch reverse osmosis. *Water Res.* **137**, 384–394. https://doi.org/10.1016/J.WATRES.2018.01.060.

Yaranal, N. A., Kumari, S., Narayanasamy, S. & Subbiah, S. 2020 An analysis of the effects of pressure-assisted osmotic backwashing on the high recovery reverse osmosis system. *J. Water Supply Res. Technol. AQUA* **69**, 298–318. https://doi.org/10.2166/AQUA.2019.089.

Zhang, P., Knötig, P., Gray, S. & Duke, M. 2015 Scale reduction and cleaning techniques during direct contact membrane distillation of seawater reverse osmosis brine. *Desalination* **374**, 20–30. https://doi.org/10.1016/J.DESAL.2015.07.005.

First received 14 December 2022; accepted in revised form 7 April 2023. Available online 9 May 2023